Application of Large Ceramics Structures to Steel Manufacturing Machinery

Application of Large Ceramics Structures to Steel Manufacturing Machinery

Nao-Aki Noda, Kyusyu Institute of Technology, Japan, noda@mech.kyutech.ac.jp
Yoshikazu Sano, Kyusyu Institute of Technology, Japan
Yasushi Takase, Kyusyu Institute of Technology, Japan
Wenbin Li, Kyusyu Institute of Technology, Japan
Hiromasa Sakai, Kyusyu Institute of Technology, Japan

Abstract: Large ceramics structures may be useful for several situations in steel manufacturing machinery because of their high abrasion and corrosion resistances. In this study, new roll structure is considered where a ceramics sleeve is connected with steel shafts at both ends by shrink fitting, which can be used in the continuous pickling line. Here, the ceramics sleeve may provide a longer lifetime and reduces the cost for the maintenance. However, attention should be paid to the maximum tensile stresses appearing between the ceramics sleeve, spacer rings and steel shafts because the fracture toughness, plasticity and fatigue strengths of ceramics are extremely lower than the values of steel. In this study, therefore, finite element method analysis is applied to the new structure, and the maximum tensile stress and stress amplitude have been investigated with varying the dimensions of the structure. Both of static and fatigue strengths of ceramics are considered under several geometrical conditions. It is found that the large ceramics structures are suitable for several steel manufacturing rolls.

1. Introduction

In steelworks, steel manufacturing machinery produces heavy plates, hot-rolled strips, cold-rolled strips, which are used in a broad range of the fields, such as automobiles, electrical appliances, and steel frames for construction. Steel manufacturing machinery includes several types of rolls and rollers, which are used in severely corrosive atmosphere. The first example is found in sink and support rolls used in molten zinc bath to manufacture zinc coated steel sheet. The second example may be seen in conveying rollers used in hot rolling line to transport hot strip. Since those rolls and rollers are used under high temperature and corrosive atmosphere, abrasion and corrosion easily arise on their surfaces in a short period. Therefore, instead of stainless steel rolls and rollers, ceramics rolls and rollers are recently considered to be used (Noda et al., 2008, 2009, 2010; Li, 2011). Since the ceramics has high heat resistance and abrasion resistance (Iwata et al., 1983), the exchanging cycle of roll and roller can be extended in a large scale.

In this paper, we will focus on the third example in continuous pickling line. Then, the application of ceramics rolls will be considered in the following sections.

2. Ceramics Structures Suitable for Continuous Picking Line

Pickling is the process of chemically removing oxides and scale from the surface of a metal by the action of water solutions of inorganic acids. Considerable variation in type of pickling solution, operation and equipment is found in the industry. Among the types of pickling equipment may be mentioned the batch picklers, modified batch, non-or

Received: 23 November 2011, Accepted: 25 November 2011
Available online 28 November 2011

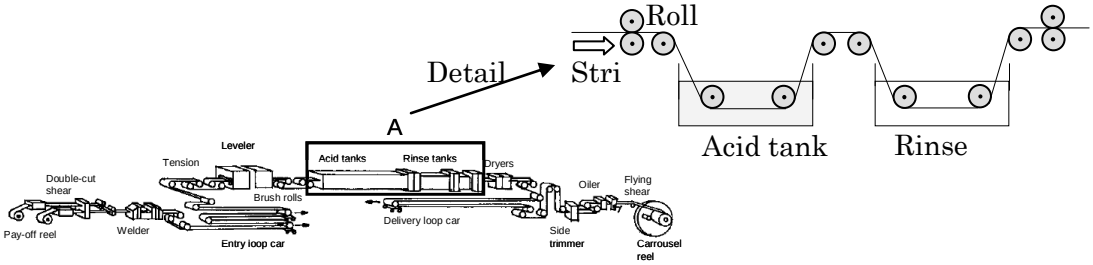

Fig.1 Schematic diagram of continuous picking line

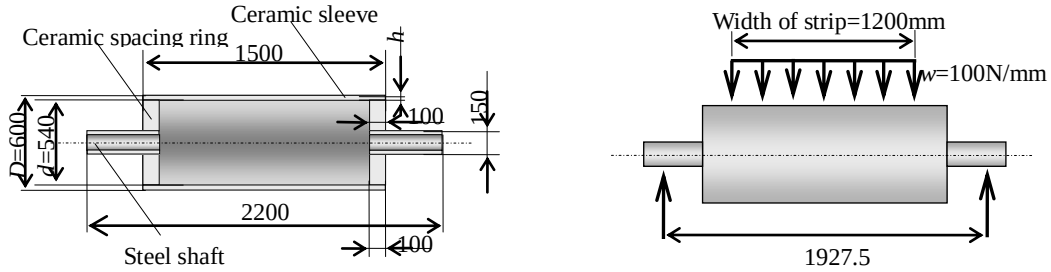

(a) Dimensions (b) Boundary conditions

Fig.2 New ceramics roll system (mm)

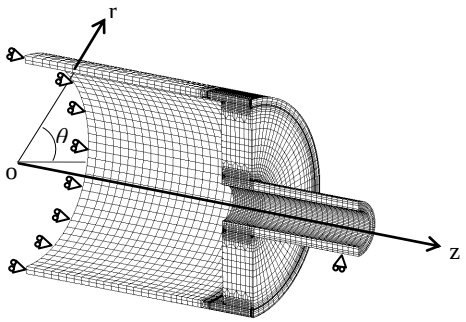

Fig.3 FEM model mesh

Table1 Material properties

	Ceramics (Si_3N_4)	Steel (Hv220)
Young's moduls (MPa)	300	210
Poisson's ratio	0.28	0.3
Tensile strength (MPa)	500	600
Fracture toughness (MPa√m)	7	100
Fatigue strength (MPa)	200	300

semi-continuous and continuous picklers (US Patent 5412966). Figure 1 shows the schematic diagram of pickling line. As shown in Fig. 1 the continuous acid wash equipment makes the coil surface beautiful by going through hydrochloric acid wash tank and removing scale layers formed on the surface in previous process. Similar lines for Fig. 1 may be found in coil painting equipment, which continuously paints the cold rolling lamina coil, the galvanizing steel board coil, and the aluminum coil, etc. on the materials, and manufactures the coated steel panel. A lot of big rolls are used for those equipments.

Currently, cast iron, carbon steel, and alloy steel are used as roll materials in those coil painting and continuous acid wash equipment, which results in wear on the roll surface in a short period. Therefore, the production lines have to be stopped to exchange the rolls requiring a lot of time for maintenance.

Here, the damage portions are usually repaired using the flame spray coating (Miki, 1989). Figure 2 shows the structure of the rolls. In this study, we will focus on the roll structure where a sleeve and two short shafts are connected by shrink fitting at both ends, and shaft and flange are connected by welding as shown in Fig.2. The use of ceramics and cemented carbide is recently promoted because they provide

high temperature resistance, high abrasion resistance and anti-oxidation. Here, we consider ceramics sleeve and ceramics spacer rings to reduce cost for maintenance.

However, to design the hollow rolls as shown in Fig. 2, attention should be paid to the maximum tensile stresses and stress amplitude appearing at the edge of the sleeve (Harada et al., 1991). In particular, since fracture toughness and fatigue strengths of ceramics are extremely smaller, stress analysis for the roll becomes more and more important compared with the cases for steel rolls. Therefore, in this study FEM analysis will be applied to the structure as shown in Fig.3, and suitable dimensions will be discussed.

3. Analytical Conditions

Define the shrink fitting ratio as δ/d, where δ is the diameter difference with the diameter d. Assume that the roll is subjected to distributed load w=12000kgf and simply supported at both ends (see Fig.2). The friction coefficient between sleeve and shafts is assumed as 0.3.

Table 1 shows the material properties of ceramics and steel. Stainless steel is usually used for rolls but ceramics roll may provide a longer maintenance span due to their high corrosion resistance and high abrasion resistance.

Figure 3 shows the finite element mesh model of the rolls. The total number of elements is 42920 and the total number of nodes is 53382. The model of 1/4 of the roll is considered due to symmetry.

4. Static Strength Analysis

4.1 Maximum Tensile Stress

We will consider the range of shrink fitting ratio $\delta/d \leq 0.3\times 10^{-3}$ because large values δ/d is not suitable for ceramics. Figure 4 shows stress distribution σ_θ at the shrink fitting ratio δ/d=0.3×10^{-3} and h=30mm. Figure 4(a) shows the stress $\sigma_{\theta s}$ due to shrink fitting and Fig.4(b) shows maximum stress distribution $\sigma_{\theta\max}(=\sigma_{\theta s}+\sigma_{\theta b})$ due to load distribution w=12000kgf after shrink fitting. As shown in Fig. 4(a), the maximum tensile stress at point A and A' are 94.52MPa while shrink fitting. It becomes 92.70MPa by applying the distribution load after shrink fitting at point A and 93.88MPa at point A' as shown in Fig. 4(b). Maximum stress after applying the load distribution 96.60MPa appears at point B also shown in Fig.4(b).

4.2 Effect of Shrink Fitting Ratio and Bending Moment upon the Maximum Tensile Stress $\sigma_{\theta\max}$

Figure 5(a) shows the relationship between $\sigma_{\theta s}$ and $\sigma_{\theta max} = \sigma_{\theta s} + \sigma_{\theta b}$ vs. δ/d when the load distribution w =12000kgf is applied after shrink fitting. When δ/d is small, the effect of stress concentration at the end of contact area is large and the effect decreases with shrink fitting ratio. From Fig.5 (a) it is found that has a minimum value at about $\delta/d = 0.1\times10^{-3}$ when h = 30mm. When, $\delta/d \geq 0.1\times10^{-3}$ $\sigma_{\theta max}$ increases linearly. In addition, $\sigma_{\theta s}$ increases linearly with increasing δ/d at h = 30mm. On the other hand, $\sigma_{\theta b}$ decreases with increasing δ/d as shown in Fig.5(b). Moreover, it is found that the large δ/d reduces the contact stress $\sigma_{\theta b}$ by gripping the shaft tightly as shown in Fig.5(b). It may be concluded that $\sigma_{\theta max} = \sigma_{\theta s} + \sigma_{\theta b}$ has a minimum value at a certain value of δ/d, which is because the stress $\sigma_{\theta s}$ increases monotonously with increasing δ/d but $\sigma_{\theta b}$ decreases.

4.3 Effect of Thickness h on $\sigma_{\theta b}$

Figure 6 shows $\sigma_{\theta b} = \sigma_{\theta max} - \sigma_{\theta s}$ vs. δ/d relation when the load distribution w = 12000kgf is applied after shrink fitting for different thickness h. Here, we assume the thickness as h =10mm, h =20mm and h =30mm. From Fig.6, it is found that stress $\sigma_{\theta b}$ decreases with increasing sleeve thickness h. Also, when h =20mm and 30mm, $\sigma_{\theta b}$ becomes constant value over the threshold value of δ/d. That means, when the δ/d is large enough, the spacer rings and sleeve can be treated as a unit body bonded perfectly (Noda et al., 2008). Figure 7 shows the relationship between the contact area ratio S_r/S_a and shrink fitting ratio δ/d. Here, S_r is the real contact area after applying load, and S_a is the apparent contact area. From the comparison between Fig.6 and Fig.7, it is found that, when h =20mm and 30mm, the threshold values coincide each other for providing the constant $\sigma_{\theta b}$ and $S_r/S_a = 1$.

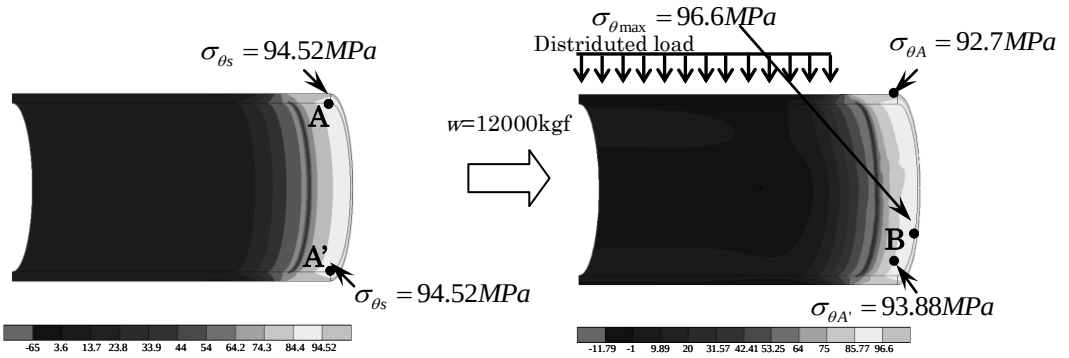

(a) σ_θ due to shrink fitting (b) σ_θ due to shrink fitting and load distribution

Fig.4 Stress distribution on the sleeve when $\delta / d = 0.3\times10^{-3}$

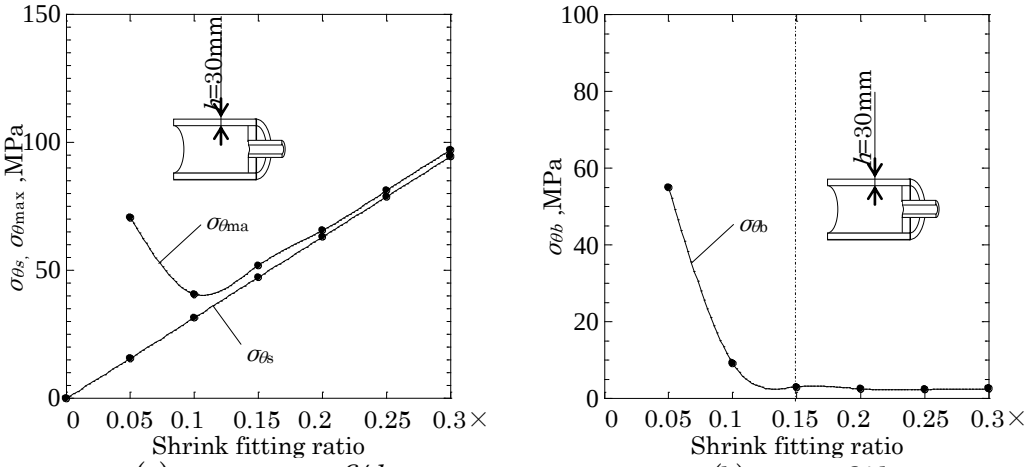

(a) $\sigma_{\theta\max}$, $\sigma_{\theta s}$ vs. δ/d (b) $\sigma_{\theta b}$ vs. δ/d

Fig.5 σ_θ vs. δ/d when h=30mm ($\sigma_{\theta\max}=\sigma_{\theta s}+\sigma_{\theta b}$)

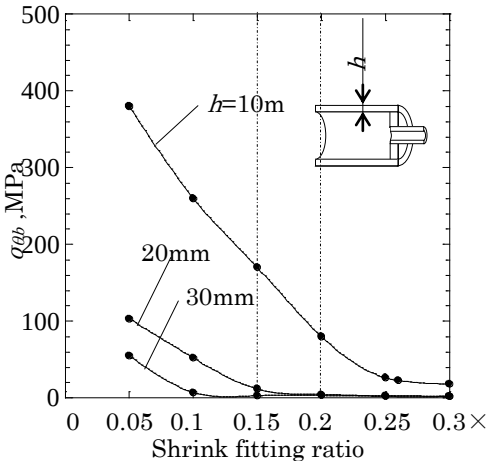

Fig.6 σ_θ vs. δ/d when h=10mm, 20mm, 30mm ($\sigma_{\theta\max}=\sigma_{\theta s}+\sigma_{\theta b}$)

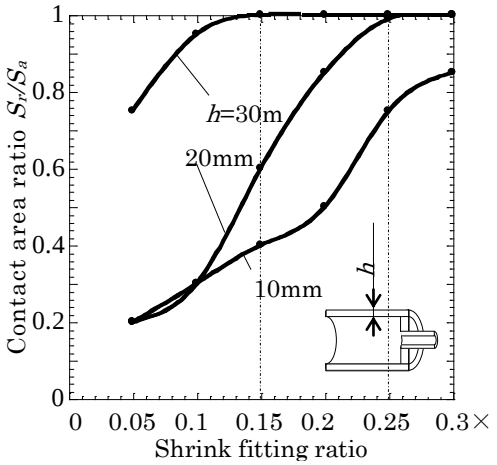

Fig.7 Contact area ratio S_r/S_a vs. δ/d when h=10mm, 20mm, 30mm
(S_r: Real contact area after applying load,
S_a: Apparent contact area)

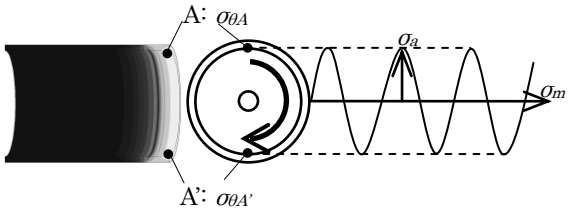

Fig.8 Cycle stress model

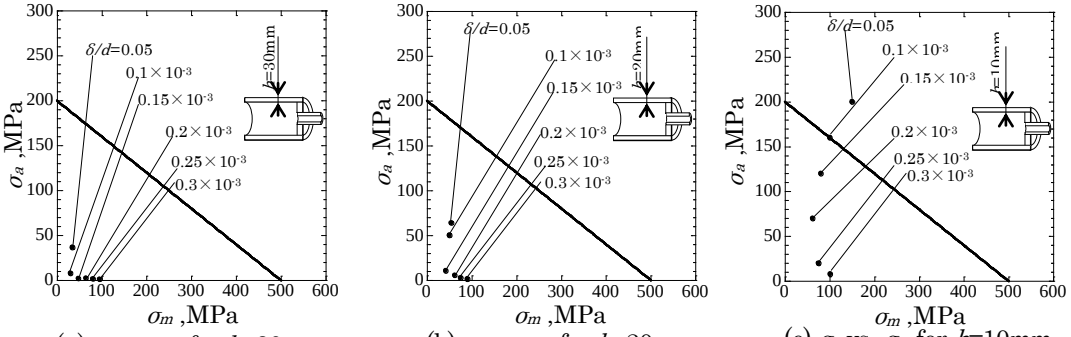

(a) σ_a vs. σ_m for h=30mm (b) σ_a vs. σ_m for h=20mm (c) σ_a vs. σ_m for h=10mm

Fig.9 Relationship between endurance limit and mean stress when h=10mm, 20mm, 30mm (Safety factor =1.0)

5. Fatigue Strength Analysis of Ceramics Rolls

Fatigue strengths analysis is important for ceramics rolls. Figure 8 shows the mean stress $\sigma_m = (\sigma_{\theta A} + \sigma_{\theta A'}) / 2$ and stress amplitude $\sigma_a = (\sigma_{\theta A} - \sigma_{\theta A'}) / 2$ at shrink fitting ratio $\delta/d = 0.3\times10^{-3}$ when thickness h = 30mm. Due to the rotation of rolls, the values of maximum stress σ_θ at the upper and lower inside of sleeve are different as shown in Fig.8 by applying load after shrink fitting. With increasing the shrink fitting ratio δ/d, the mean stress increases and the stress amplitude decreases. As shown in Figure 9, the values of stress amplitude σ_a and mean stress σ_m are below the fatigue strengths of ceramics material. In other words, the fatigues strength can be larger by applying larger shrink fitting ratio.

6. Conclusion

In this paper, the application of ceramics rolls was considered by taking an example of continuous picking line in steel manufacturing machinery. In order to reduce maintenance cost for exchanging the rolls, a new structure was considered where a ceramics sleeve connected with ceramics spacer ring and steel shafts at both ends by shrink fitting. Maximum tensile stress and fatigue strength analysis were performed by the application of the finite element method; then several geometrical conditions were investigated, such as thickness of the sleeve. The conclusions can be made in the following way.

(1) The maximum tensile stress appears at the inner surface of the sleeve at the right end as σθmax. The stress σθmax can be expressed as $\sigma_{\theta max} = \sigma_{\theta s} + \sigma_{\theta b}$ where $\sigma_{\theta s}$ is the stress due to shrink fitting and $\sigma_{\theta b}$ is the stress due to load distribution. For example, the maximum tensile stress due to shrink fitting at point A and A' are 94.52MPa when $\delta/d=0.3\times10^{-3}$ at h=30mm. It becomes 92.70MPa by applying the distribution load after shrink fitting at point A and 93.88MPa at point A'. The maximum tensile stress after applying load distribution is 96.60MPa appearing at point B.

(2) For small values of δ/d, the maximum stress $\sigma_{\theta max}$ becomes larger because large contact forces may appear between the sleeve and space rings, especially for small thickness. Appropriately large values of δ/d may reduce $\sigma_{\theta max}$ effectively. In other words, $\sigma_{\theta max}$ has a minimum

value at a certain value of δ/d.

(3) The effect of thickness of the sleeve was considered. Under small values of δ/d, a large thickness of the sleeve may reduce $\sigma_{\theta b}$ because the sleeve clamps the space rings more tightly and reduces the magnitude of contact forces. On the other hand, large values of δ/d with large thickness of sleeve may increase the value of $\sigma_{\theta b}$.

(4) Fatigue strength analysis is very important for ceramics rolls subjected to load distribution. Fatigue strength can be decreased by reducing the shrink fitting ratio.

References:

Harada, S., Noda, N., Uehara, O., and Nagano, M. (1991). "Tensile strength of hot isostatic pressed silicon nitride and effect of specimen dimension." Transactions of the Japan Society of Mechanical Engineering, Vol.57, No.539, 1991, 173-178.

Iwata, T., and Mori, H. (1983). "Material choice for hot run table roller." Plant Engineer, Vol.15, No.6, 1983, 55-59 (in Japanese).

LI, W., Noda, N. A., Sakai, H., and Takase, Y. (2011). "Analysis of Separation Conditions for Shrink Fitting System Used for Ceramics Conveying Rollers." Journal of Solid Mechanics and Material Engineering, Vol.5, No.1, 2011, 14-24.

Miki, E. (1989). "High corrosion resistance and cost reduction by spraying methods." Plant Engineer, Vol.21, No.1, 1989, 8-12 (in Japanese)

Noda, N. A., Hendra., Takase, Y., and Tsuyunaru, M. (2008). "Maximum stress for shrink fitting system used for ceramics conveying rollers." Journal of Solid Mechanics and Material Engineering, Vol.2, No.11, 2008, 1410-1419.

Noda, N. A., Yamada, M., Sano, Y., Sugiyama, E., and Kobayashi. S. (2008). "Thermal stress for all-ceramics rolls used in molten metal to produce stable high quality galvanized steel sheet." Engineering Failure Analysis, Vol.15, 2008, 261-274.

Noda, N. A., Hendra., Takase, Y., and LI, W. (2009). "Thermal stress analysis for ceramics stalk in the low pressure die casting machine." Journal of Solid Mechanics and Material Engineering, Vol.3, No.10, 2009, 1090-1100.

Noda, N. A., Hendra., Takase, Y., Ogura, H., and Higashi, Y. (2010). "Thermal stress and heat transfer coefficient for ceramics stalk having Protuberance dipping into molten metal." Journal of Solid Mechanics and Material Engineering, Vol.4, No.8, 2010, 1198-1213.

US Patent 5412966, "Push-pull pickle line, Available." from <www.freepatentsonline.com>.